

RESEARCH

Open Access



# Structural Behavior of Spliced Post-Tensioned Girders with Precast Box Segments

Min Sook Kim and Young Hak Lee\*

## Abstract

It is widely known that the precast segment method facilitates quality control and reduces the costs as well as the construction period. The method, however, has limited applicability since it causes structurally unstable behaviors due to stress concentration in the joints. Against this backdrop, this paper suggested precast segment joints for the improved structural performance and experimentally evaluated the structural performance of the proposed joints in terms of crack pattern, mode of failure, strain, maximum load and displacement ductility. In order to improve constructability as well as structural performance, this paper suggests joints combined with shear key, post tension and steel rod and conducts static load tests. The test results showed that, in terms of maximum load capacity, the resistance of a girder where shear key and post tension are applied to joint details stood at around 86.4% of a monolithic girder's and demonstrated better ductility behaviors than the monolithic girder.

**Keywords:** precast concrete, post-tension, splice sleeve, shear key, spliced girder

## 1 Introduction

The precast segmental construction has been widely used in bridge construction due to many advantages such as excellent durability, low life-cycle costs, and quality control since the late 1960s. The precast concrete segment (PCS) method is widely applied to building structures now as it ensures the high quality and reduces the construction period by minimizing on-site placement work (Wium and Buyukozturk 1984). However, the joints of the spliced girders represent locations of discontinuity through which compression and shear forces are transmitted. The stiffness of the joint can be weaker than those of monolithic girders (Wium and Buyukozturk 1984; Zhou et al. 2005). Nevertheless, there is little information not only on the behaviors and design methods of PCS-applied structures but also the joints between segments that play a significant role in these PCS-applied structures (Zhou et al. 2005).

Finding it crucial to apply the shear key which ensures high shear resistance and ductility due to transversal interlocking, Zhou et al. (2005) conducted tests with the number of shear keys and the use of epoxy coating on the joint surfaces as variables to analyze effects of individual variables and propose a formula for calculating the shear strength of shear key. Buyukozturk et al. (1990) also considered segment joints as the most important element throughout design and construction, and evaluated the shear strength and deformation of joints through tests on the use of shear key and epoxy and the level of prestressing as variables. Miller et al. (1999) performed tests considering the location of shear key and grouting material as variables that can control the crack of shear key.

Tadros et al. (1993) suggested two new methods of connection: one is by using jacking bracket and mechanical splice in pre-tensioned/post-tensioned precast concrete system to connect spliced girder; the other is by applying spacer strut and jacking bracket. It showed that the suggested one has more improved than the existing connection in the aspect of seismic resistance and structural integrity. Saleh et al. (1995) suggested methods: connecting precast concrete girder using high strength threaded

\*Correspondence: leeyh@khu.ac.kr  
Department of Architectural Engineering, Kyung Hee University, Yongin,  
South Korea  
Journal information: ISSN 1976-0485 / eISSN 2234-1315

rod splicing and one using pre-tensioned strand splicing. The suggested method showed that structure and economical efficiency has been better than the previous one.

Despite the PCS method has been widely applied to various construction fields, previous studies have been mainly about the application of conventional joint details to evaluate the local or global behaviors of structures or the characteristics of grouting materials, with relatively little research focused on developing enhanced joint details that can improve their structural performance.

In this paper, various types of PCS joint details to develop joint details to improve the structural performance were proposed and tested to evaluate the structural behaviors of these joint details in terms of patterns of crack and failure, maximum load resistance capacity and ductility.

## 2 Experimental Program

In order to evaluate the structural performance of the proposed PCS-based joints, five specimens were manufactured by applying the combination of post tension, steel rod and shear key. For the comparative purpose, a monolithic girder was also manufactured. The combinations of the applied joint details were presented in Table 1.

### 2.1 Specimens

Hollow sections with the external cross section of 750 mm × 750 mm and the internal section of 350 mm × 350 mm were applied to the specimens. All the specimens except the monolithic specimen were manufactured by splicing two segments with the length of 1,650 mm as presented in Fig. 1. Unlike the conventional cast-in-place method that extends rebars from each segment when splicing two segments and places concrete into the joints in construction sites to attach specimens, rebars were connected using high strength non-shrinkage mortar charging-type splice sleeves for ease of construction and the integrity of rebar splices in this study. The details of splice sleeve are shown in Fig. 2. Since it has recently been reported that multiple unreinforced

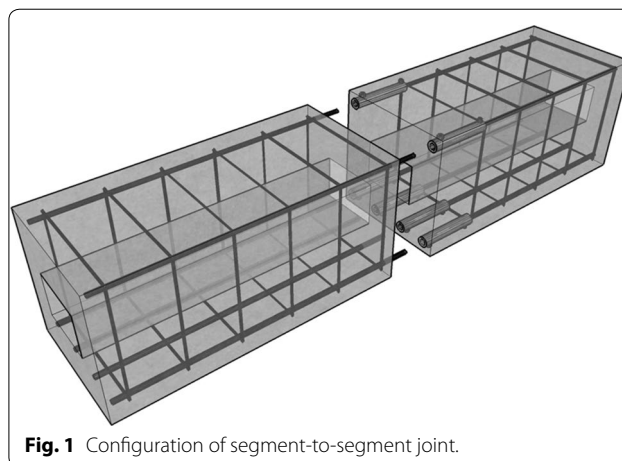


Fig. 1 Configuration of segment-to-segment joint.

concrete shear keys enhance the structural performance of joints by better interlocking than single reinforced shear key (Buyukozturk et al. 1990), the multiple unreinforced shear keys were applied to three specimens as illustrated in Fig. 3. Also, Hanna et al. (2007) conducted test and show a full-depth shear key improve a moment-resisting connection (Hanna et al. 2007).

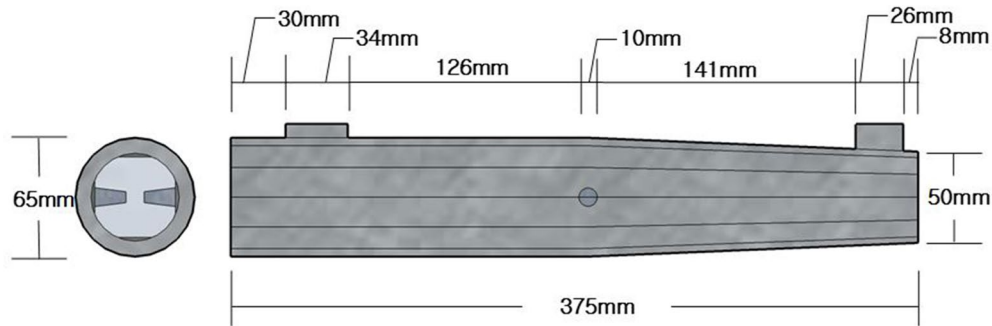
To improve splicing performance, post tensioning method was used for specimens, SGSP and SGP, and steel rods were used for specimen, SGSS. The details of each specimen are presented in Fig. 4. The manufacturing process of specimens is illustrated in Fig. 5. Epoxy was applied to the joint surfaces of the specimens with thickness of 2 mm after the removal of the forms. The rebars of these segments were inserted into one side of splice sleeve, and non-shrinkage mortar was injected into splice sleeve holes for the first joints. Then, steel rod or post tensioning was applied to create the second joints depending on which splicing method was used. As for post tensioning specimens, jacking force of 128.5 kN was applied. As shown Fig. 6, in the case of a steel rod-applied specimen, the hole was set up in the segment in advance to insert steel rod and to fasten the bolt of steel rod before concrete placing. After inserting steel rod into segment which exposed steel bar, steel bar was put into spliced sleeve; steel rod was inserted in the hole on the other side to set up steel rod then it was assembled with the other segment. Later, bolts were fastened in both ends of steel rods then non-shrinkage mortar was placed in the space which previously had been set up for fastening the bolts.

### 2.2 Materials

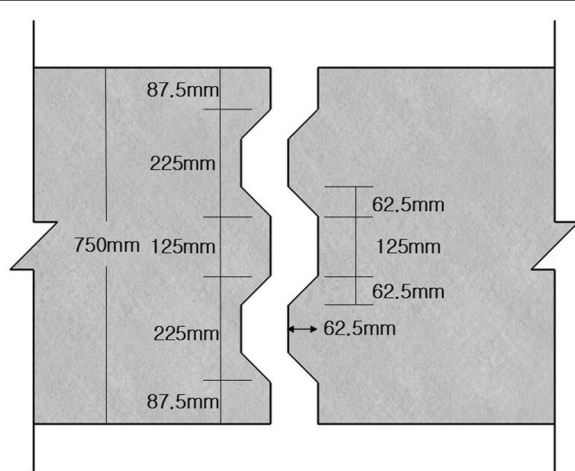
The 28-day compressive strength of concrete of the specimens was evaluated from a standard cylinder test. The average concrete compressive strength was 45.2 MPa.

Table 1 Test variables.

Specimen	Joint type
MG	Monolithic girder
SGSP	Splice girder + shear key + post-tension
SGP	Splice girder + post-tension
SGSS	Splice girder + shear key + steel rod
SGS	Splice girder + shear key
SG	Splice girder



**Fig. 2** Splice sleeve.



**Fig. 3** Details of shear keys.

The sizes of rebars used for longitudinal reinforcements and stirrups are 25 and 10 mm, respectively, and their tensile strength is 400 MPa. The diameter of steel rods was 28 mm with tensile strength of 400 MPa. Material properties of steel strands and splice sleeves used for the

test are summarized in Tables 2 and 3, respectively. Also, the properties of the steel rods are presented in Table 4.

### 2.3 Test Setup

To assess the structural performance of the proposed joints, the specimens were the simply supported and loaded as shown in Fig. 7a. Linear variable differential transformers (LVDTs) were placed on a half span to measure vertical displacements. During the fabrication of the specimen, strain gauges were attached at the center of top and bottom bars as shown in Fig. 7b.

## 3 Test Results

### 3.1 Crack and Failure Modes

Figure 8 shows cracks at 80% of the maximum load for the test specimens; a thick continuous line exhibits joint separation mode. Initial flexural cracks occurred at mid-span in all specimens. As load increased, the crack patterns were various depending on the joint details. For MG specimen, the initial flexural cracks were propagated into the compression zone and shear cracks occurred as the loading increased as shown Fig. 8a. Openings of

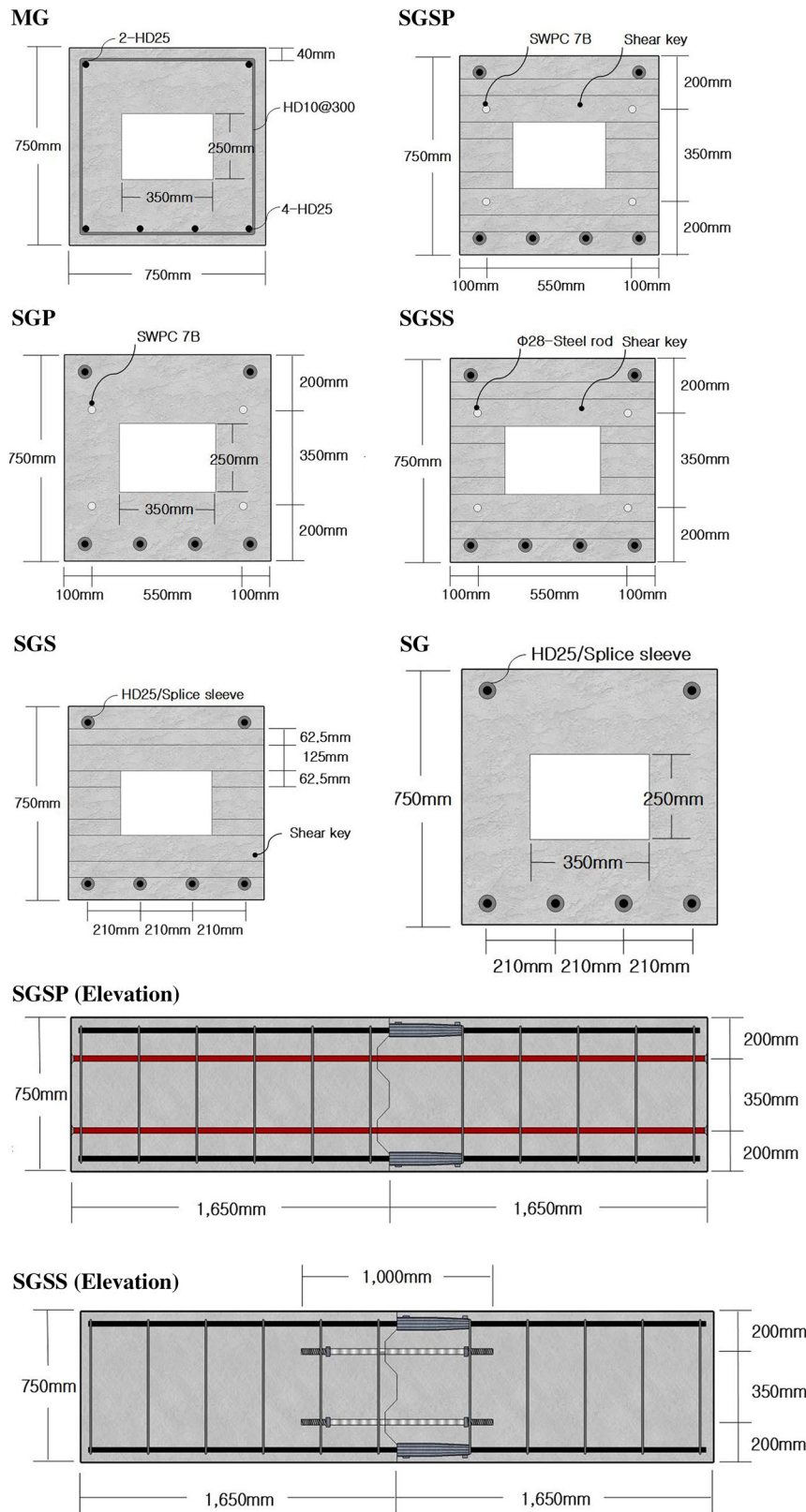


**Fig. 4** Details of specimens.



SG and SGS specimen occurred after the initial flexural cracks as shown in Fig. 8b, c. For SGS specimen, cracks occurred at the midspan were developed up to the top fiber of the specimen as the loading increased.

Also, opening of SGP specimen occurred after the initial flexural cracks occurred as the loading increased. Its crack patterns were similar to SG specimen as shown in Fig. 8d. SGSP and SGSS specimens showed the similar

crack patterns to that of MG specimen. For SGSP specimen, the initial flexural cracks were propagated into the compression zone and these cracks were extended to the upper shear key of the joint as shown in Fig. 8e. Severe spallings occurred in SGSS specimen as cracks were developed. And the cracks occurred at the shear key root at the bottom were propagated to upper shear key as shown in Fig. 8f. In SGSP and SGSS specimens, flexural

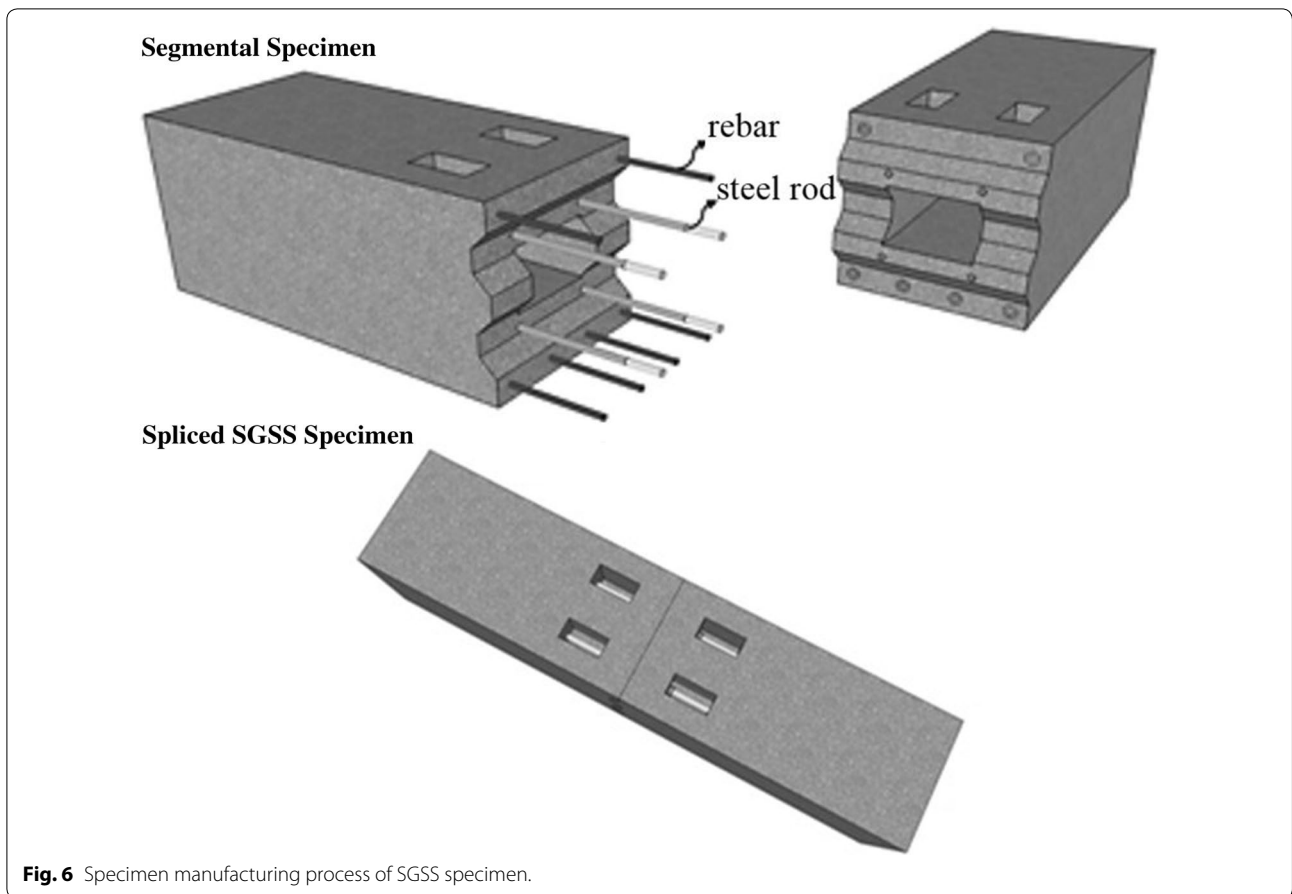


**Fig. 6** Specimen manufacturing process of SGSS specimen.

**Table 2** Material properties of strands.

Type	Diameter (mm)	Area (mm <sup>2</sup> )	Unit weight (kg/km)	Elongation (%)
SWPC7B	12.7	98.7	774	3.5

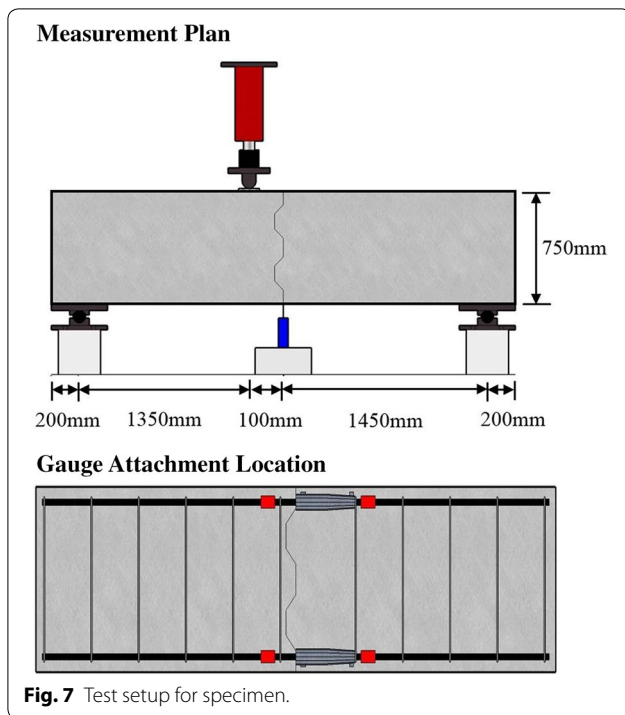
**Table 3** Material properties of splice sleeves.

Type	Yield strength (MPa)	Tensile strength (MPa)	Modulus of elasticity (GPa)	Elongation (%)
GCD50	414	562.1	166.8	16.0

**Table 4** Material properties of steel rods.

Type	Diameter (mm)	Area (mm <sup>2</sup> )	Yield strength (MPa)	Tensile strength (MPa)
SS400	28	615.8	250	400

and diagonal cracks were developed similar to those of MG specimen. This shows that two spliced segments experienced even distribution of stress and made the similar behaviors to the monolithic girder as the integrity of joint was achieved. SG and SGS specimens failed at relatively lower loads than the other specimen because of rapid joint openings, thus they experienced fewer cracks. Except MG specimen, all the others experienced joint opening and ultimate failure. At the load of 401.4 kN, initial flexural cracks occurred in the bottom center of MG specimen. Then the specimen failed due to the flexural shear cracks at the maximum load of 884.8 kN. The failure mode is presented in Fig. 9a. SGSP specimen experienced a temporary loss of load due to joint opening at 320.6 kN, but the loading was kept increased on a stable basis afterwards. Cracks were developed in the shear keys at the load of 683.1 kN, and the load kept fluctuating—even after reaching the maximum load—without undergoing a sharp decrease. Then the load declined gradually as the opening of joints increased as shown in Fig. 9b. After bottom bar slips occurred in SGSS specimen, a number of cracks were developed than the other specimens, and spallings took place as the width



of these cracks grew. Then it reached the maximum load of 581.6 kN where compression failure of concrete occurred.

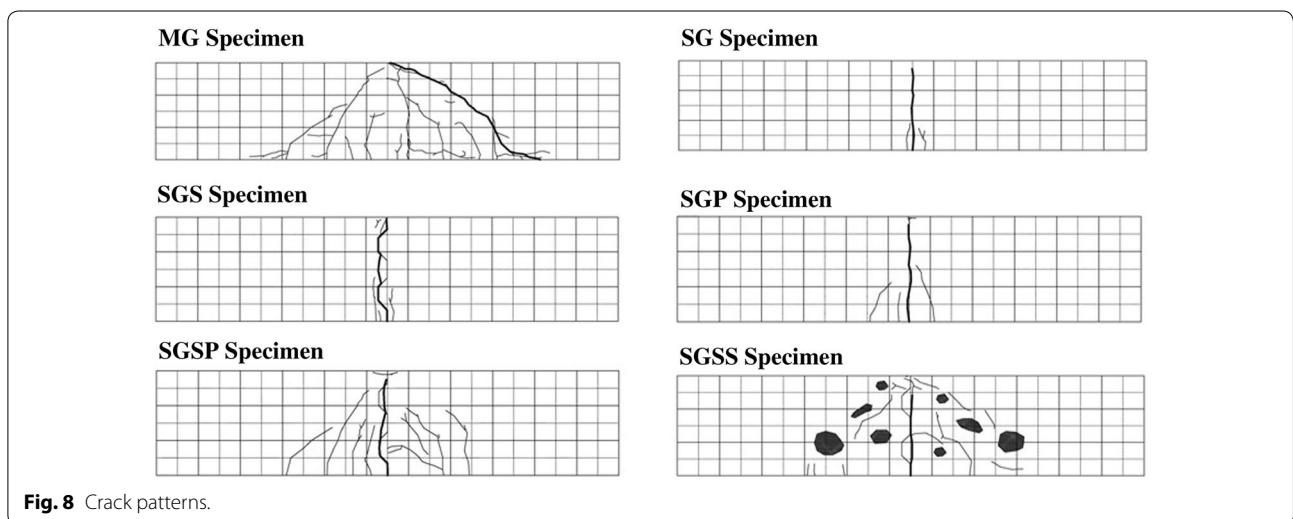
As shown in Fig. 9c, cracks occurred in the shear keys in SGP specimen, and joint opening occurred at the load of 302.2 kN. Then, as the opening of joints became wider at 504.6 kN, the friction between the steel strand and

concrete generated noise, which was followed by anchorage failure and strand rupture (Fig. 9d).

The load of the specimen declined as joint opening became gradually wider as shown in Fig. 9e. The load of SGS specimen declined after bottom bar slips occurred at the initial stage of loading and then recovered, but it started to drop again when vertical cracks were generated in the shear keys. In the case of SG specimen, cracks were found in the epoxy-bonded area at the load of 192.4 kN. Then bottom bar slips took place at 220.2 kN, initiating joint opening; as the bottom bar slips increased at the load of 290.3 kN, the specimen's load diminished sharply compared to SGS specimen.

### 3.2 Strain and Load–Displacement Relations

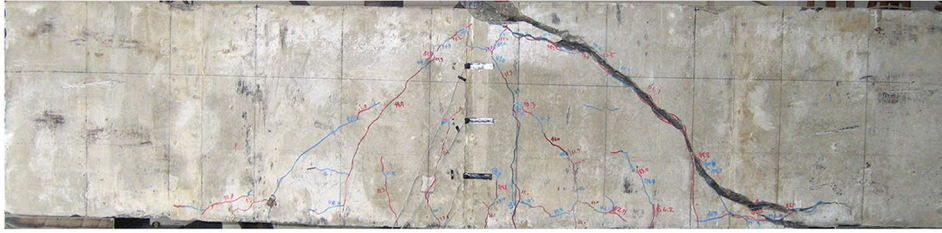
As shown in Fig. 10a, the bars strain of SGSP specimen increased dramatically at a lower level of load compared to MG specimen. This is because segmental specimens experience stress concentration compared to the monolithic girder throughout which stress is evenly distributed. In Fig. 10b, the strain of reinforcements in SGSP specimen was similar to that of MG specimen, while reinforcements in SGS specimen showed a low strain, as joint failures took place before applied load was evenly distributed throughout the specimen. In other words, the joint details of SGSP specimen outperform SGS specimen's in terms of integrity due to post tensioning. The test results are summarized in Table 5 and the load–displacement relations of individual specimens are presented in Fig. 11. The five segmental joint specimens showed similar behaviors with MG specimen until the



(See figure on next page.)

**Fig. 9** Failure modes.

**MG Specimen**



**Joint Opening (SGSP)**



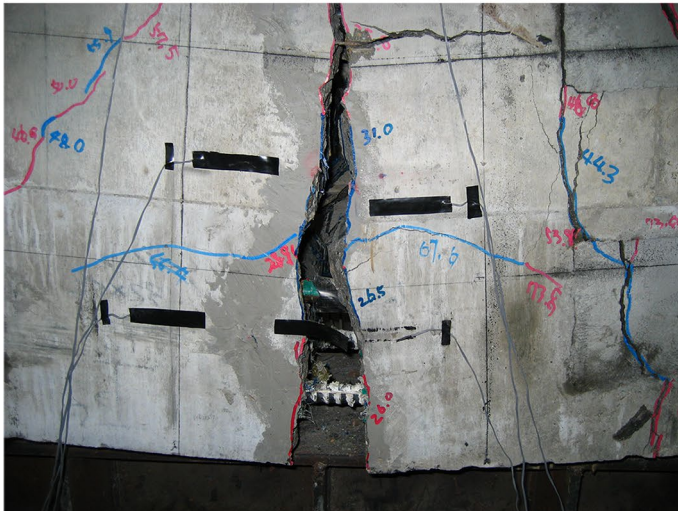
**Shear Key Crack**



**Steel Strand Breakage**



**SGP Specimen**



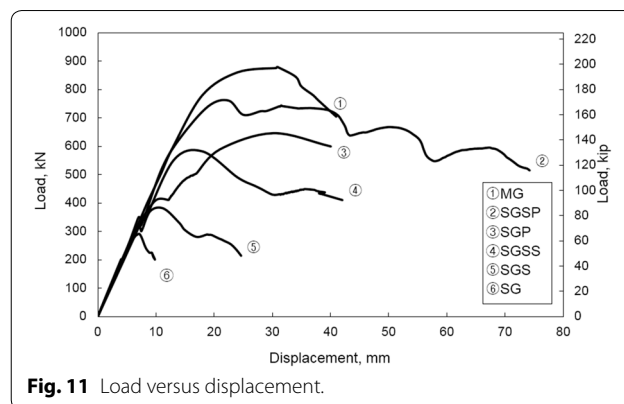
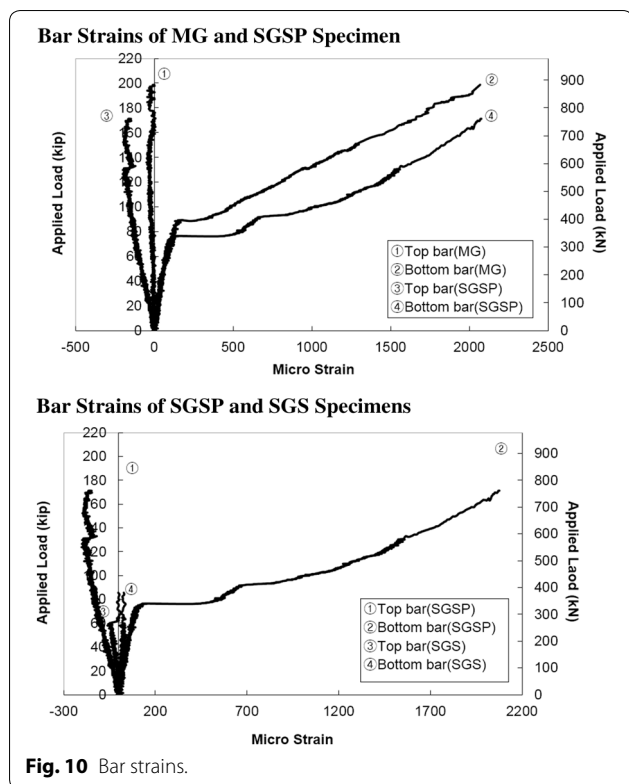


Fig. 11 Load versus displacement.

approximately twice of that of SGS specimen which had the same joint details as SGSP but the post-tensioning because the post-tensioning improved the load transfer between the segments as well as the integrity of the segments. Comparing with the specimen SGSS, SGSP specimen had about 178 kN larger the maximum load. Though both the post-tensioning and the steel rods improved the integrity of the segments, the post-tensioning applied specimen showed the larger load resistance capacity because wider cracks and severe spallings of concrete occurred to the specimen SGSS and its effective sectional area was being reduced dramatically in consequence.

Table 5 Test results.

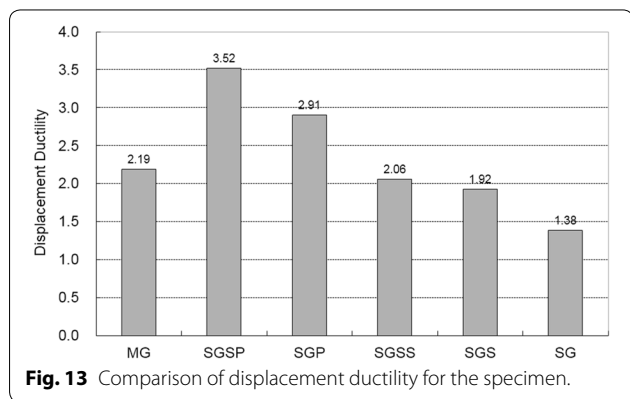
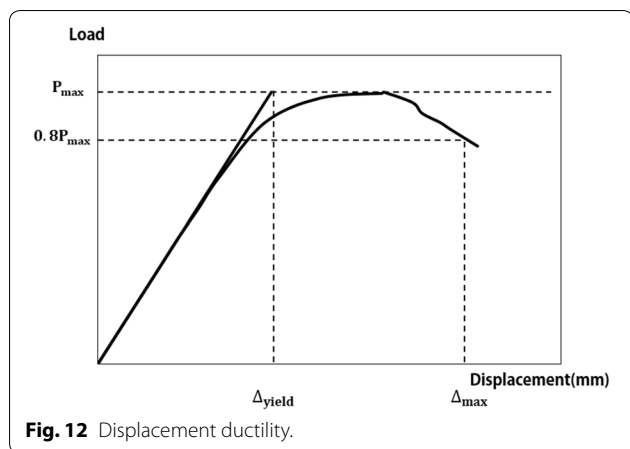
Specimen	$P_{max}$ (kN)	$\delta$ (mm)	$\Delta_{max}/\Delta_{yield}$
MG	879.6	30.86	2.19
SGSP	760.1	22.5	3.52
SGP	646.7	30.15	2.91
SGSS	581.6	18	2.06
SGS	380	11.3	1.92
SG	290.7	7.12	1.38

slips of bottom bars; their levels of initial stiffness were also similar to MG specimen's. Except for MG specimen, others experienced a temporary drop in loads when the bottom bar slip occurred, and their loads bounced back to reach the maximum loads.

As shown in Fig. 11 and Table 5, in terms of the effect of shear key, SGS specimen had about 89 kN larger load resistant capacity than SG specimen which had no shear key but the other figurations were the same as SGS. Also, SGSP specimen had approximately 103 kN larger load resistance than SGP specimen. This is because that the shear key plays a role of mechanical interlock. In terms of the effect of post-tensioning, the maximum load of SGSP specimen showed

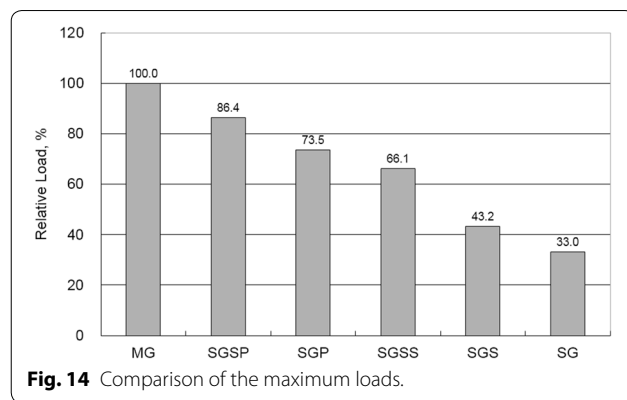
### 3.3 Evaluation of Displacement Ductility and Maximum Load Resistance Capacity

In order to evaluate the ductility performance of the drop as ultimate displacement. As for SGP specimen, specimens with the various joint details, the displacement ductility index ( $\mu$ ), the ratio of ultimate displacement ( $\Delta_{max}$ ) to yield displacement ( $\Delta_{yield}$ ) was used in the paper. As it is difficult to estimate the accurate yield displacement ( $\Delta_{yield}$ ) in load–displacement relations, this study adopted the method suggested by Sheikh as shown in Fig. 12. Sheikh and Khoury (1997) defined the displacement when specimen reaches the maximum load while maintaining initial stiffness as yield displacement and the displacement at 80% of the maximum loads after the load begins to however, the displacement when the steel strand failed was used in calculating the displacement ductility since it was not possible to obtain the data from the maximum load to 80% of that load due to strand breakage and anchorage failure. The displacement ductility indexes of the specimens were presented in Fig. 13. Comparing with MG specimen, SGSP and SGP specimen showed approximately 1.6 and 1.3 times higher ductility indexes, respectively. Also, the displacement ductility indexes of post tension-applied SGP and SGSP



specimens are around 1.4 times and 1.7 times higher than the SGSS specimen's. Shear key-applied SGS specimen showed approximately 1.4 times higher index than SG specimen and the displacement ductility index of a shear key-applied SGSP specimen is around 1.2 times higher than that of an SGP specimen. SGSP specimen to which both post-tensioning and shear key were applied showed the highest ductility index of 3.52. The use of post tension and shear key, therefore, is believed to play an integral role in improving the ductility behaviors of joints.

Figure 14 summarizes the resistance levels of individual spliced girders with various joint details by the ratio of the maximum load to that of the monolithic girder. The maximum loads of SGSP and SGP specimens stand at 86.4% and 75.3% of MG specimen's, respectively. This indicates that the behaviors and load resistant capacities of the two specimens are comparable to that of a monolithic girder, ensuring the integrity of joints. SG and SGS specimens spliced only with splice sleeve, on the other hand, fell short of MG specimen's maximum load.



### 4 Summary and Conclusions

In this paper, five spliced girders with various joint details were tested to evaluate the structural performance in terms of the integrity and the ductility. For the comparison, one monolithic girder was manufactured. The following conclusions are drawn based on the test results obtained:

1. The test results on SG specimen showed that spliced precast box girder with splice sleeve and epoxy only had insufficient structural capacity in terms of maximum load and displacement ductility.
2. In the case of SGSP specimens to which shear key and post tension are applied, their loads kept fluctuating without any dramatic decline in loads after reaching the maximum load. Also, it showed the most excellent structural performance in terms of the displacement ductility index and the maximum load capacity among the spliced specimens.
3. As for SGSS specimen spliced with steel rods, constructability would likely be high upon on-site application because its assembling process was relatively simpler than the other joints tested in this paper. The test results presented, however, that cracks became wider and severe spalling took place as loads increased comparing with the other specimens.
4. Among the joints tested in this paper, the load resistance capacity of shear key- and post tension-applied SGSP joints was around 86.4% of the monolithic girder, and it showed better ductility behavior than the monolithic girder.

#### Authors' contributions

MS performed experiment and analyzed data regarding the post-tensioned spliced girder. YH analyzed the experimental data and was a major contribution in writing the manuscript. Both authors read and approved the final manuscript.

**Acknowledgements**

This work was supported by the National Research Foundation of Korea (NRF) grant funded by the Korea government (MSIT) (NRF-2017R1A2B2005581).

**Competing interests**

I confirmed that I have read Springer Open's guidance on competing interests and have included a statement indicating that none of the authors have any competing interests in the manuscript.

**Availability of data and materials**

The datasets used and/or analysed during the current study are available from the corresponding author on reasonable request.

**Funding**

Funder: National Research Foundation of Korea. Award number: NRF-2017R1A2B2005581.

**Publisher's Note**

Springer Nature remains neutral with regard to jurisdictional claims in published maps and institutional affiliations.

Received: 13 November 2018 Accepted: 31 December 2018

Published online: 20 March 2019

**References**

- Buyukozturk, O., Bakhom, M. M., & Beattie, S. M. (1990). Shear behavior of joints in precast concrete segmental bridges. *Journal of Structural Engineering, ASCE*, 116(12), 3380–3401.
- Hanna, K. E., Morocous, G. and Tadros, M. K. (2007) Transverse design and detailing of adjacent box beam bridges. In *Proceedings, PCI National Bridge Conference*, Phoenix, AZ.
- Miller, R. A., Hlavacs, G. M., Long, T., & Grueuel, A. (1999). Full-scale testing of shear keys for adjacent box girder bridges. *PCI Journal*, 44(6), 80–90.
- Saleh, M. A., Einea, A., & Tadros, M. K. (1995). Creating continuity in precast girder bridges. *Concrete International*, 17(8), 27–32.
- Sheikh, S. A., & Khoury, S. S. (1997). A performance-based approach for the design of confining in tie columns. *ACI Structural Journal*, 94(4), 421–431.
- Tadros, M. K., Ficenec, J. A., & Einea, A. (1993). A new technique to create continuity in prestressed concrete members. *PCI Journal*, 38(5), 30–37.
- Wium, D. J. W., & Buyukozturk, O. (1984). Precast segmental bridge-status and future directions. *Civil Engineering for Practicing and Design Engineers, ACSE*, 3, 59–79.
- Zhou, X., Mickleborough, N., & Li, Z. (2005). Shear strength of joints in precast concrete segmental bridges. *ACI Structural Journal*, 102(1), 3–11.